

Article

Optimization Research on Burner Arrangement of Landfill Leachate Concentrate Incinerator Based on “3T+E” Principle

Wangsong Wu ^{1,*}, Jiajin Liu ^{2,3}, Shuya Guo ⁴, Zhukai Zeng ¹, Guangyao Cui ^{2,3} and Zhongqing Yang ^{2,3,*}¹ Powerchina Zhongnan Engineering Corporation Limited, Changsha 410014, China² Key Laboratory of Low-Grade Energy Utilization Technologies and Systems, Chongqing University, Ministry of Education, Chongqing 400044, China³ School of Energy and Power Engineering, Chongqing University, Chongqing 400044, China⁴ School of Mathematics and Big Data, Chongqing University of Arts and Sciences, Chongqing 402160, China

* Correspondence: 02340@msdi.cn (W.W.); zqyang@cqu.edu.cn (Z.Y.)

Abstract: At present, the treatment of landfill leachate is an unavoidable challenge facing environmental problems. Incineration is one of the effective methods to treat landfill leachate which meets the 3T+E principle and can avoid the production of dioxin in the process of treatment. Based on the 3T+E principle, this paper studied the influence of burner arrangement on the treatment of landfill leachate through the numerical simulation method. The research showed that the symmetrical arrangement of reverse swirl and same direction flow were more conducive to the combustion of landfill leachate concentrations in the incinerator so that the residence time of the flue gas in the second combustion chamber can also exceed 2 s. When the nozzle arrangement height is 0.9 m–0.8 m, the wall collision rate of concentrated liquid droplets can be reduced, and the burnout rate of landfill leachate was the highest, reaching more than 92%.

Keywords: landfill leachate; waste liquid incineration; numerical simulation; incinerator



Citation: Wu, W.; Liu, J.; Guo, S.; Zeng, Z.; Cui, G.; Yang, Z.

Optimization Research on Burner Arrangement of Landfill Leachate Concentrate Incinerator Based on “3T+E” Principle. *Energies* **2022**, *15*, 5855. <https://doi.org/10.3390/en15165855>

Academic Editor: Albert Ratner

Received: 16 July 2022

Accepted: 10 August 2022

Published: 12 August 2022

Publisher’s Note: MDPI stays neutral with regard to jurisdictional claims in published maps and institutional affiliations.



Copyright: © 2022 by the authors. Licensee MDPI, Basel, Switzerland. This article is an open access article distributed under the terms and conditions of the Creative Commons Attribution (CC BY) license (<https://creativecommons.org/licenses/by/4.0/>).

1. Introduction

Landfill leachate [1–6] contains high concentrations of organic matter, inorganic pollutants, pathogens, corrosive acid, ammonia, nitrogen, heavy metals, foreign matter, inorganic salts, etc. [7–10]. Toxicological tests have confirmed that landfill leachate has mutagenic, teratogenic and carcinogenic effects on bacteria, algae, invertebrates and fish [11], and as the landfill time increases, the organic matter in the landfill leachate becomes more complex and difficult to deal with [12]. One of the evaluation criteria for landfill leachate treatment is the “3T+E” principle (temperature, time, turbulence and excess air, that is, when the temperature of the flue gas in the secondary combustion chamber or the flue before entering the waste heat boiler is not lower than 850 °C and the temperature of the flue gas in the furnace and secondary combustion chamber is no less than 2 s, there is sufficient turbulent intensity in the furnace and appropriate excess air coefficient).

The arrangement of the burner has a very important influence on the combustion efficiency of the reactor [13–15]. Rohini’s [16] results show that different burner arrangement affects the uniform temperature distribution in the combustion space and the effective heating of combustion gas. Li [17] used a new burner arrangement scheme, which can improve the aerodynamic field in the furnace and improve the combustion efficiency of coal. Liu [18] found that in the methanol reforming burner, the 45° + 60° blade angle arrangement has the best combustion characteristics. Ghasemi’s [19] research shows that the asymmetric burner arrangement can improve the heat transfer coefficient and Nussel number of the burner.

At present, incineration is one of the effective methods to treat landfill leachate, and its core idea is to thoroughly reduce the amount of landfill leachate through high-temperature combustion. Ehrhardt [20] carried out combustion experiments on an industrial-scale waste

liquid incineration device. The experimental results show that when the temperature is higher than 900 °C, due to the fast oxidation kinetics of carbon monoxide and hydrocarbons, the combustion process is only affected by the evaporation efficiency of the waste liquid. When the temperature is lower than 850 °C, the combustion process is not only affected by the evaporation efficiency of waste liquid but also limited by chemical kinetics. Bai [21] put forward the strategy of treating waste liquid with a cement rotary kiln as a zero emission strategy, calcined the waste liquid, and evaluated its impact on products by characterizing the mineral phase and strength of cement clinker. The results show that after adding waste liquid, the main phase and strength of cement clinker have little difference, and the burnability of raw meal was improved. The waste liquid can be used as an alternative fuel in actual production. Liu's experimental [22] results show that the higher the ash content, the lower the concentration of polyfluoroalkyl substances (PFAS) in the leachate when the ashes of municipal solid waste incineration are treated together with the landfill leachate. Zhang's experimental results show that COD in waste liquid is degraded fastest in the temperature range of 600–1000 °C, while NH₃-N is degraded fastest in the temperature range of 400–800 °C. In addition, oxygen concentration and residence time also have a certain impact on the degradation rate of COD and NH₃-N [23].

To sum up, the feasibility of using the incineration method to treat the landfill leachate has been verified by some scholars. Using this method to treat landfill leachate can effectively remove toxic and harmful substances in landfill leachate, and the incineration method, as a fully quantitative treatment method, will not leave secondary pollution products such as concentrate or sludge. This paper takes a large landfill as an example. The treatment capacity of the landfill leachate concentrate is 2 t/h. The incineration process of the landfill leachate concentrate after precipitation and concentration is mainly studied. The biogas generated by the landfill is used for auxiliary landfill leachate combustion. In addition, this paper optimizes the atomization and combustion process of landfill leachate concentrate in the furnace so that the combustion process meets the "3T+E" principle, and the feasibility of its treatment method is improved.

2. Methods

2.1. Physical Model

The incineration method of landfill leachate concentrate is to spray the leachate into the incinerator through the atomizing nozzle after precipitation and concentration, and then evaporate and burn it with the help of combustion-supporting biogas. The whole combustion process is a complex, multi-relative heat and mass transfer process. Due to the complexity of the actual process, some necessary simplifications have been made on this basis. The model of the landfill leachate concentrate incinerator used in this paper is shown in Figure 1. The combustion-supporting biogas is sent into the furnace by the swirl burner and is fully mixed and burned under the action of swirl wind, providing conditions for the evaporation and combustion of landfill leachate concentrate. The concentrated liquid is sprayed into the furnace from the front end of a combustion chamber by an atomizing nozzle, and the evaporation combustion process is completed in the first combustion chamber. Finally, all combustion products enter the second combustion chamber and finally enter the flue.

The overall design of the landfill leachate concentrate incinerator meets the requirements of 75–100 kW/m³ of furnace volume thermal intensity in burner area, as required in *Boiler Principle and Calculation*, and the thermal intensity of furnace section in burner area does not exceed 4.6 MW/m². After accounting, the size of the incinerator was finally determined as shown in Figure 2, with the length of L (L = 4 m) and located at the X axis. The width is W (W = 3 m), located in the Z axis, and the height of the whole incinerator is H (H = 3 m), of which the height of the first combustion chamber is H₁ (H₁ = 1.5 m), and the height of the second combustion chamber is H₂ (H₂ = 1.3 m), which is located on the Y axis. According to the calculation, the thermal strength of the furnace volume of the landfill

leachate concentrate incinerator is 90.45 kW/m^3 , and the thermal strength of the furnace section is 542.68 kW/m^2 , which meets all design requirements.

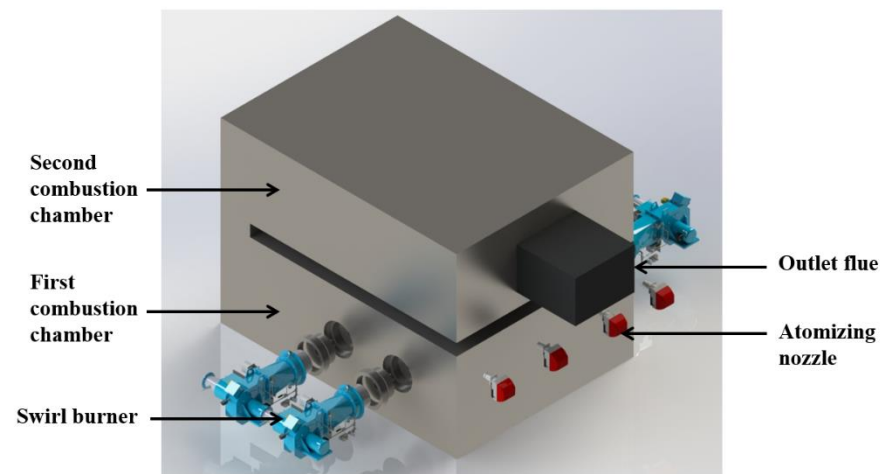


Figure 1. Three-dimensional model of the incinerator for the landfill leachate concentrate.

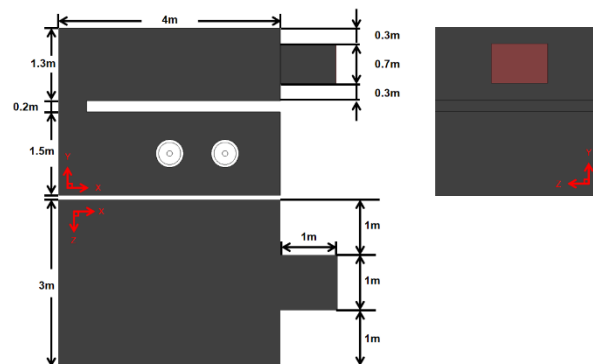


Figure 2. Three views of landfill leachate concentrate incinerator.

The incinerator adopts swirl burners. In order to increase the turbulence intensity of air flow in the furnace, the burners were arranged symmetrically in the same direction of swirl, symmetrically in the opposite direction of swirl and staggered in the same direction of swirl. The four swirl burners are arranged on both sides of the first combustion chamber, with an arrangement height of 0.75 m and a spacing of 1 m between the two burners, which meets the burner spacing index in *the design manual of oil and gas fired boilers*. For the convenience of subsequent description, the parameters are described here. Figure 3 is a three-dimensional view of the landfill leachate concentrate incinerator, showing the direction of the three-dimensional coordinate axis in the incinerator. The incident position of landfill leachate concentrate is indicated, which is located on the wall of $X = 4 \text{ m}$. The nozzle arrangement height is the vertical distance from the incident position of the nozzle to the wall of $Y = 0 \text{ m}$.

In the “3T+E” principle, the excess air coefficient and turbulence intensity are qualitative indicators which are not easy to evaluate, while the residence time and outlet flue gas temperature are quantitative indicators, so this paper mainly evaluates the residence time and outlet flue gas temperature under working conditions.

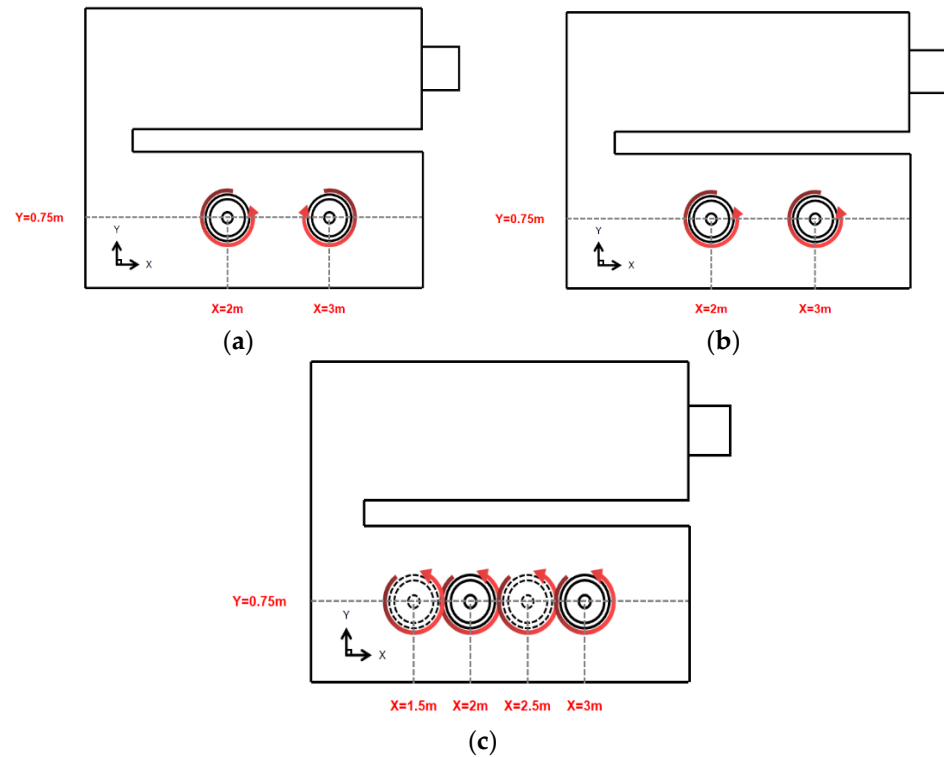


Figure 3. Three different burner arrangement modes and relative swirl direction. (a) Symmetrical arrangement of burners with reverse swirl. (b) Symmetrical arrangement of burners with same direction flow. (c) Burner-staggered arrangement with same direction flow.

2.2. Mathematical Model

In this paper, the combustion process of landfill leachate concentrate in the incinerator was studied, which can be regarded as a fluid system with radiation heat transfer and combustion reaction. The governing equations are as follows:

(1) Continuity equation:

$$\frac{\partial \rho}{\partial t} + \frac{\partial}{\partial x_j}(\rho u_j) = S_m \tag{1}$$

In the formula, t is the time (s), u_j is the velocity vector and S_m is the mass added to the continuous phase from the dispersed secondary phase, which in this context refers to the evaporation of landfill leachate concentrate droplets.

(2) Momentum equation:

$$\frac{\partial}{\partial t}(\rho u_i) + \frac{\partial}{\partial x_j}(\rho u_i u_j) = -\frac{\partial p}{\partial x_i} + \frac{\partial \tau_{ij}}{\partial x_j} + \rho g_i + F_i \tag{2}$$

In formula, ρ , u and p represent the density, velocity and static pressure, respectively, τ_{ij} is the stress tensor, ρg_i and F_i are the gravitational body force and the external body force, respectively, in the i direction.

(3) Energy equation:

$$\frac{\partial}{\partial t}(\rho E) + \frac{\partial}{\partial x_i}(u_i(\rho E + p)) = \frac{\partial}{\partial x_i} \left(k_{eff} \frac{\partial T}{\partial x_i} - \sum_{j'} h_{j'} J_{j'} + u_j (\tau_{ij})_{eff} \right) + S_h \tag{3}$$

ρ and u represent the density and velocity of the gas phase, respectively, P and τ_{ij} represent the pressure and shear stress tensors and $E = h - \frac{p}{\rho} + \frac{V^2}{2}$ represents the total energy of the fluid micelles, that is, the sum of internal energy and kinetic energy. k_{eff} is the effective heat conductivity, $k_{eff} = k_t + k$. J_j' is the diffusion flow of component j' . The first three terms on the right in the equation describe the energy transport caused by heat conduction, component diffusion and viscous dissipation, respectively, meaning exothermic and endothermic, due to the chemical reaction.

(4) Turbulence equation:

$$\frac{\partial}{\partial t}(\rho k) + \frac{\partial}{\partial x_i}(\rho k u_i) = \frac{\partial}{\partial x_i} \left(\left(\mu + \frac{\mu_t}{\sigma_k} \right) \frac{\partial k}{\partial x_j} \right) + G_k + G_b - \rho \varepsilon - Y_M + S_k \quad (4)$$

$$\frac{\partial}{\partial t}(\rho \varepsilon) + \frac{\partial}{\partial x_j}(\rho \varepsilon u_j) = \frac{\partial}{\partial x_j} \left(\left(\mu + \frac{\mu_t}{\sigma_\varepsilon} \right) \frac{\partial \varepsilon}{\partial x_j} \right) + \rho C_1 S_\varepsilon - \rho C_2 \frac{\varepsilon^2}{k + \sqrt{\nu \varepsilon}} + C_{1\varepsilon} \frac{\varepsilon}{k} C_{3\varepsilon} G_b + S_\varepsilon \quad (5)$$

$$C_1 = \max \left[0.43, \frac{\eta}{\eta + 5} \right] \quad (6)$$

$$\eta = S \frac{k}{\varepsilon} \quad (7)$$

In the formula, G_k is the turbulent kinetic energy due to laminar velocity gradient, G_b is the turbulent kinetic energy due to buoyancy, Y_m is the fluctuation due to excessive diffusion in compressible turbulent flow, C_2 and $C_{1\varepsilon}$ are empirical constants and σ_k and σ_ε are the k equations and the Prandtl number for turbulent flow of the ε equation.

2.3. Discretization Method and Boundary Conditions

This paper adopted a solver based on pressure/velocity. In order to study whether the incinerator conforms to the predetermined "3T+E" principle after stabilization, the steady-state solver was selected. The selected mathematical model was relatively simple, and the coupled algorithm has advantages in solving the incompressible flow of rotating motion and has good stability. Therefore, the coupled algorithm was selected. The structure of the model is simple, so the hexahedral mesh, which has obvious advantages over tetrahedral mesh in computing speed, was used to generate meshes with a total number of about 140,000–820,000. Shown in Figure 4 are the meshes of the landfill leachate concentrate incinerator.

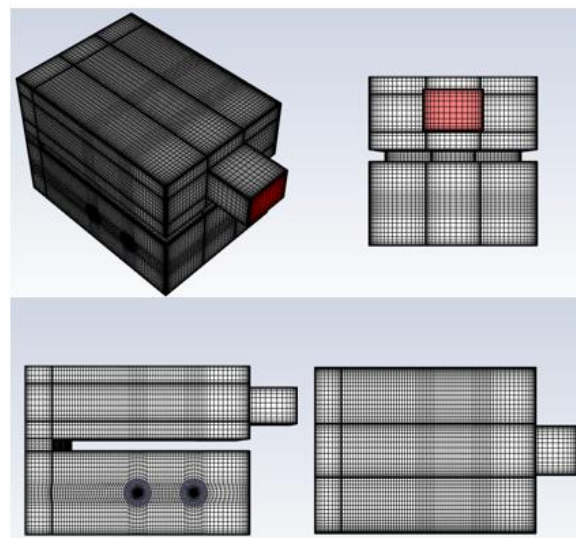


Figure 4. Incinerator mesh structure diagram.

In the design of the concentrated liquid incineration process in the incinerator, the gas–liquid, two-phase swirl and combustion reaction and the number of meshes affect the calculation results to a certain extent. In order to avoid the influence of meshes on the calculation results, this paper verifies the meshes with a total of 140,000; 260,000; 350,000; 460,000; 600,000 and 820,000 sizes detecting the speeds at different positions of the second combustion chamber, as shown in Figure 5. With the increase in the number of meshes, the speed of the detection points corresponding to 460,000–820,000 meshes basically changes little. In order to save computing resources, the 460,000 meshes were finally selected for numerical calculation.

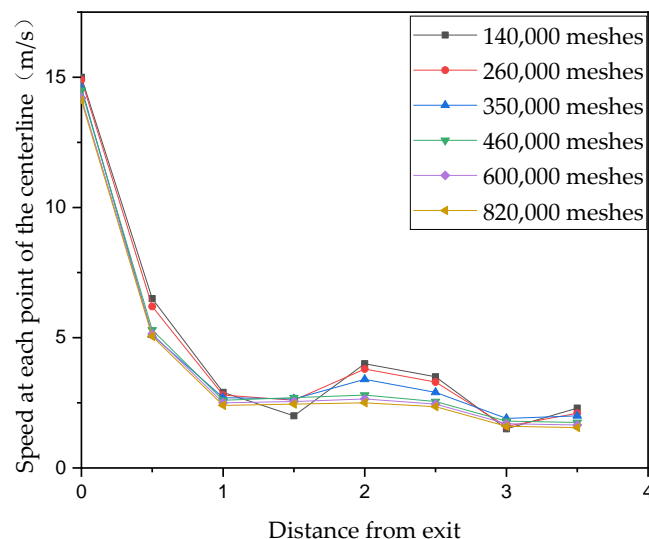


Figure 5. Speed of mesh detection points with different sizes.

The parameters of burner inlet and landfill leachate concentrate are shown in Table 1.

Table 1. Gas–liquid two-phase flow parameters.

Flow Field	Item	Unit	Design Condition
Gas phase	Air	N ₂ volume fraction	% 79
		O ₂ volume fraction	% 21
	Combustion-supporting biogas	CH ₄ volume fraction	% 60
		CO ₂ volume fraction	% 40
	Burner swirl air inlet velocity	Axial speed	m/s 2
		Tangential velocity	m/s 1
	Burner direct flow air inlet velocity	Inlet speed	m/s 5
	Burner combustion-supporting biogas inlet speed	Axial speed	m/s 8
Tangential velocity		m/s 5	
Calorific value		kJ/kg 3652.6	
Moisture content (mass fraction)		% 76.25	
Liquid phase	Nozzle form	Solid cone	
	Spray direction	Perpendicular to the wall and facing the furnace	
	The average particle size	um	150
	Jet velocity	m/s	18
	Single-nozzle flow	kg/s	0.139

3. Results and Discussion

3.1. Combustion Characteristics of Landfill Leachate under Different Burner Arrangements

Figure 6 shows the complete burnout ratio of the concentrate in the incinerator under the three burner arrangements. It can be seen that when the burner arrangement is symmetrical, the burn-up ratio of the concentrated liquid in the incinerator is more than 92%, no matter whether the adjacent burners are reverse swirl or same direction swirl, and most of the concentrated liquid has completed the evaporative combustion process. However, when the burners are arranged in a staggered arrangement with co-rotating flow, the burnout ratio of the concentrate drops slightly to only 87.5% because some of the concentrate fails to complete its evaporation and combustion processes.

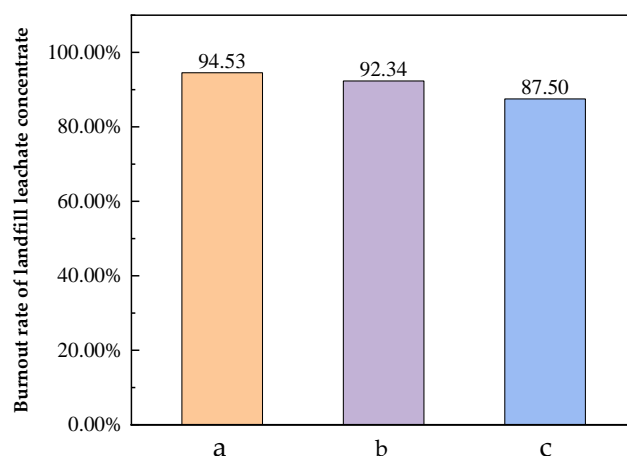


Figure 6. The complete combustion ratio of concentrated liquid under three different burner arrangements: (a) symmetrical arrangement of burners with reverse swirl; (b) symmetrical arrangement of burners with same direction flow; (c) burner-staggered arrangement with same direction flow.

This is because when the burner is arranged in a hedging arrangement, the airflow collides and burns at the center of a combustion chamber, and a part of the flue gas forms a backflow flue gas. However, the incident droplets just meet the backflow flue gas, and the velocity of the droplets in the X direction are reduced by the influence of the backflow flue gas; when the velocity of some droplets in the X direction is reduced to zero, they flow to the lower half of the combustion chamber (Y direction), but the flame direction is upward, the temperature of the lower half of the combustion chamber is lower, the heat transfer driving force of the droplets in this area is also lower and the heat absorption and evaporation ratio is slower. As a result, some of the droplets hit the wall at the bottom of the combustion chamber before completely evaporating.

In Figure 7, the temperature distributions of the central cross-section of a combustion chamber under three different arrangements of the burner are shown. When the burners are arranged symmetrically, regardless of the same direction or the reverse swirl flow, there is a large area of low temperature in the central cross section of a combustion chamber from $X = 2.5$ m to $X = 4$ m. This is because the concentrated liquid droplets enter the incinerator after atomization, absorb heat and evaporate in this area and then absorb a lot of heat, resulting in low temperatures in this area. At $X = 2.5$ m, most of the concentrated liquid droplets complete the evaporation process, the volatiles start to burn and release a lot of heat, and the temperature of the combustion chamber gradually increases. From $X = 0$ m to $X = 0.5$ m, the high temperature flue gas begins to transfer to the second combustion chamber, and the temperature gradually decreases. When the burner is arranged in staggered rows and swirling in the same direction, it can be clearly seen that due to the dislocation of the burner, the low-temperature zone formed by the evaporation and heat absorption of concentrated liquid droplets is more inclined to the positive direction of the Z axis at $X = 3$ m, and after the combustion of the concentrated liquid droplets, the

high-temperature flue gas flowing to the second combustion chamber is slightly inclined to the negative direction of Z the axis.

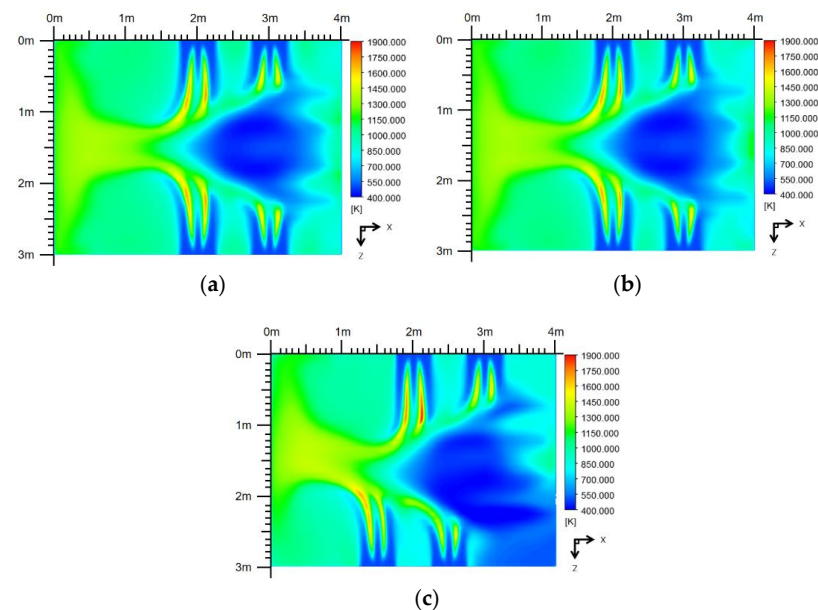


Figure 7. Temperature cloud diagram of the central cross-section of the first combustion chamber ($Y = 0.75$ m). (a) Symmetrical arrangement of burners with re-verse swirl; (b) symmetrical arrangement of burners with same direction flow; (c) burner-staggered arrangement with same direction flow.

As can be seen from Figure 8, when the burners are staggered and arranged in the same direction, the temperature distribution of the second combustion chamber is affected because the high-temperature area of the first combustion chamber is biased towards the negative direction of the Z axis, resulting in uneven temperature distribution of the second combustion chamber in the case of the staggered arrangement of burners, which easily forms a local, high-temperature area. In contrast, when the burners are symmetrically arranged, the temperature distribution in the second combustion chamber is uniform, there is no large temperature gradient, and it is not easy to form local, high temperatures.

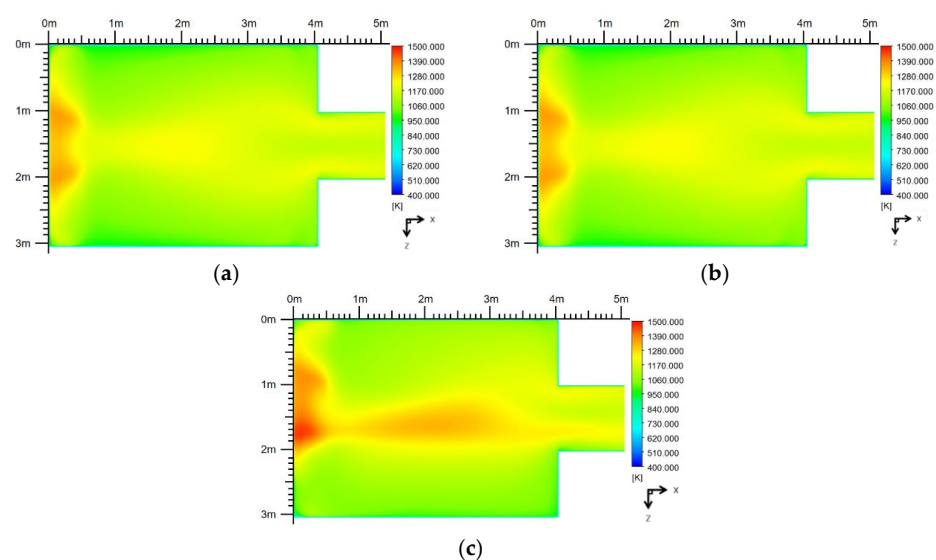


Figure 8. Temperature cloud diagram of central cross-section of the second combustion chamber ($Y = 2.35$ m). (a) Symmetrical arrangement of burners with reverse swirl; (b) symmetrical arrangement of burners with same direction flow; (c) burner-staggered arrangement with same direction flow.

Table 2 shows the residence time of the flue gas in the second combustion chamber and the temperature of the flue gas at the outlet under three different arrangements of the burner. It can be seen from the table that under the three burner arrangements, the outlet flue gas temperatures are all above 1123.15 K, which meets the outlet flue gas temperature requirements. However, when the burner arrangement is staggered and with same direction flow, due to the change of the flow field in the incinerator, the residence time of the flue gas in the second combustion chamber is too short, only 1.64 s, which does not meet the “3T+E” principle.

Table 2. Flue gas residence time and outlet flue gas temperature meter under different arrangement modes of burner.

Burner Layout		Symmetrical Arrangement of Burners with Reverse Swirl	Symmetrical Arrangement of Burners with Same Direction Flow	Burner-Staggered Arrangement with Same Direction Flow
Item	Residence time/s	2.18	2.45	1.64
	Outlet flue gas temperature/K	1152.69	1153.20	1157.87

In Figure 9, the turbulent kinetic energy of a central cross section of a combustion chamber ($Y = 0.75$ m cross section) when the burner adopts symmetrically arranged reverse swirl and symmetrically arranged with same direction flow is shown. It can be seen that when the burner adopts the symmetrical arrangement of reverse swirl and same direction flow, the turbulent kinetic energy is very close, and the maximum turbulent kinetic energy is $5.62 \text{ m}^2/\text{s}^2$ and $5.47 \text{ m}^2/\text{s}^2$, respectively. Overall, no matter which burner arrangement is used, the central cross section of the combustion chamber has strong turbulent kinetic energy.

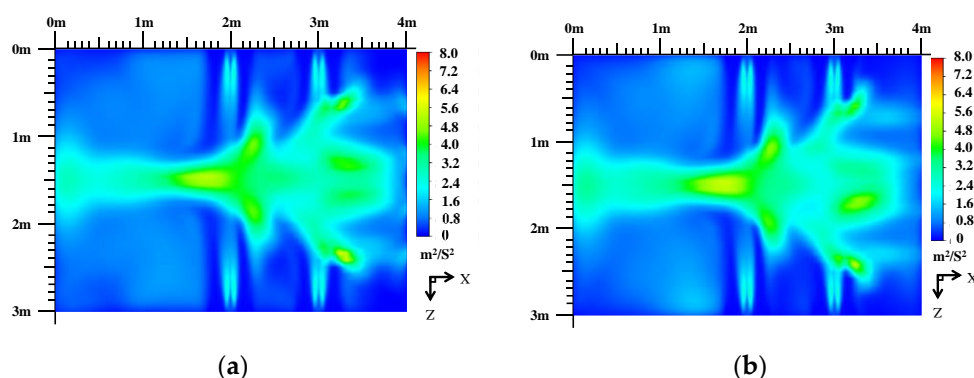


Figure 9. A cloud diagram of turbulent kinetic energy in the cross-section of the center of the combustion chamber ($Y = 0.75$ m). (a) The burner is symmetrically arranged with re-verse swirl. (b) Symmetrical arrangement of burners with same direction flow.

3.2. Influence of Nozzle Arrangement Height on Incineration Process of Landfill Leachate Concentrate

The arrangement height of atomizing nozzles has a great influence on the incineration process of the landfill leachate concentrate. The relationship between the different arrangement heights of the atomizing nozzles and the burnout ratio of the concentrated liquid when the size of the concentrated liquid droplets is 100 μm , the incident speed is 10 m/s, the atomization angle is 60° and the nozzle flow is 8.33 L/min is shown in Figure 10.

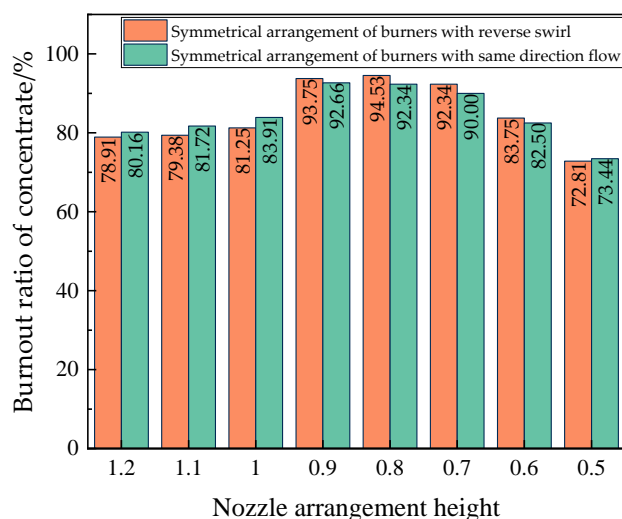


Figure 10. Burnout ratio of concentrated liquid with different nozzle arrangement heights.

It can be seen from Figure 10 that when the change law of the burnout ratio of the landfill leachate concentrate in the furnace when the burner is symmetrically arranged with reverse swirl (same direction swirl) and the nozzle arrangement height of the landfill leachate concentrate changes from 1.2 m to 0.5 m, the burnout ratio of droplets is as shown in Table 3, which shows that the burnout ratio of the concentrated liquid first increases with the decrease of nozzle arrangement height. When the arrangement height changes to 0.8 and 0.9 m, the burnout ratio reaches the peak, and then reducing the nozzle arrangement height reduces the burnout ratio the of concentrated liquid.

Table 3. The residence time of the flue gas, the burnout ratio of droplets and the outlet flue gas temperature under different nozzle arrangement heights.

Symmetrical Arrangement of Burners with Reverse Swirl								
Nozzle arrangement heights/m	1.2	1.1	1	0.9	0.8	0.7	0.6	0.5
Residence time/s	2.12	2.27	2.45	2.26	2.18	2.08	2.75	2.73
Burnout ratio of droplets	78.91%	79.38%	81.25%	93.75%	94.53%	92.34%	83.75%	72.81%
Outlet flue gas temperature/K	1150.25	1154.47	1157.87	1151.58	1152.69	1158.4	1155.94	1155.35
Symmetrical Arrangement of Burners with Same Direction Flow								
Nozzle arrangement heights/m	1.2	1.1	1	0.9	0.8	0.7	0.6	0.5
Residence time/s	2.62	2.33	2.37	2.85	2.45	2.64	2.78	2.79
Burnout ratio of droplets	80.16%	81.72%	83.91%	92.66%	92.34%	90%	82.5%	73.44%
Outlet flue gas temperature/K	1152.57	1156.58	1158.35	1150.42	1151.2	1157.44	1154.68	1157.68

Table 3 reflects the residence time of the flue gas in the second combustion chamber and the outlet flue gas temperature under different nozzle arrangement heights of droplets. It can be seen from the table that the flue gas residence time is more than 2 s, and the outlet flue gas temperature is more than 1123.15 K (850 °C), which meets the quantitative requirements for flue gas residence time and outlet flue gas temperature in the “3T+E” principle.

Figure 11 shows the cloud diagram of turbulent kinetic energy in the central cross-section of a combustion chamber at different heights. Due to the change of nozzle arrangement height, the burnout ratio of the concentrated liquid and its evaporation and combustion position in the incinerator change, which affects the turbulent kinetic energy in

the incinerator and makes it slightly different, but it can be seen that the difference is small, and the incinerators have a certain turbulence intensity.

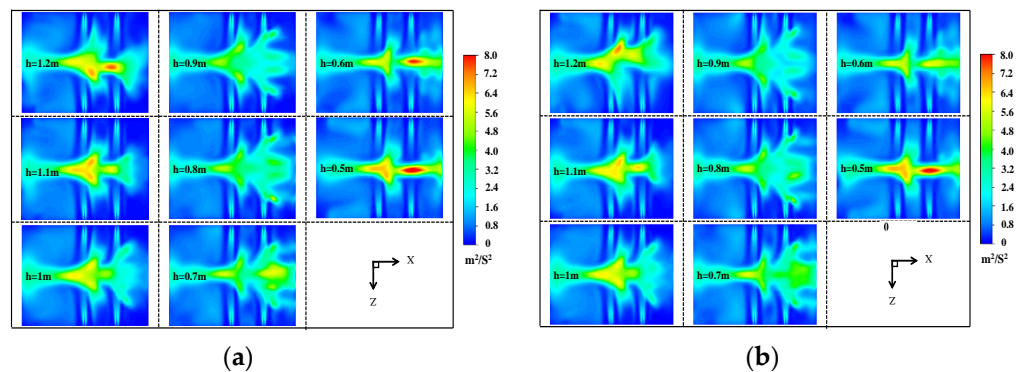


Figure 11. Turbulent energy cloud diagram of the center cross-section of the first combustion chamber under different nozzle arrangement heights ($Y = 0.75$ m). (a) The burner is symmetrically arranged with reverse swirl. (b) Symmetrical arrangement of burners with same direction flow.

In Figure 12, from the variation diagram of droplet size with trajectory under different nozzle arrangement heights, it can be seen that when the nozzle arrangement height is higher than 0.9 m, the droplet encounters strong reflux flue gas after the incident, resulting in a sharp drop in the velocity of the droplet in the X direction, and the velocity in the X direction becomes zero after moving for a short distance. Some of the low-speed liquid droplets are picked up by the return flue gas and brought to the top of the combustion chamber to impact the wall surface, while other liquid droplets are brought to the lower half of the combustion chamber by the return flue gas to complete the evaporation process or impact the wall surface of the region. With the decrease of the nozzle arrangement height until the arrangement height avoids strong reflux flue gas, when the arrangement height is 0.9–0.8 m, the incident droplets can move a long distance in the X direction, and most of the droplets can complete the evaporation process in the high-temperature area in the center of a combustion chamber. At this time, the burnout ratio of the droplets is the highest and the wall collision ratio is the lowest. However, the arrangement height is too low. For example, when the nozzle arrangement height is lower than 0.7 m, although the incident droplets can run a long distance in the X direction, under the dual action of gravity and reflux flue gas, the droplets move to the lower half of the combustion chamber. The temperature in this area is low, and the evaporation time of the droplets is long. Some droplets contact the bottom of the combustion chamber before complete evaporation, and hit the wall at the bottom. At this time, the burnout ratio of the droplets is low.

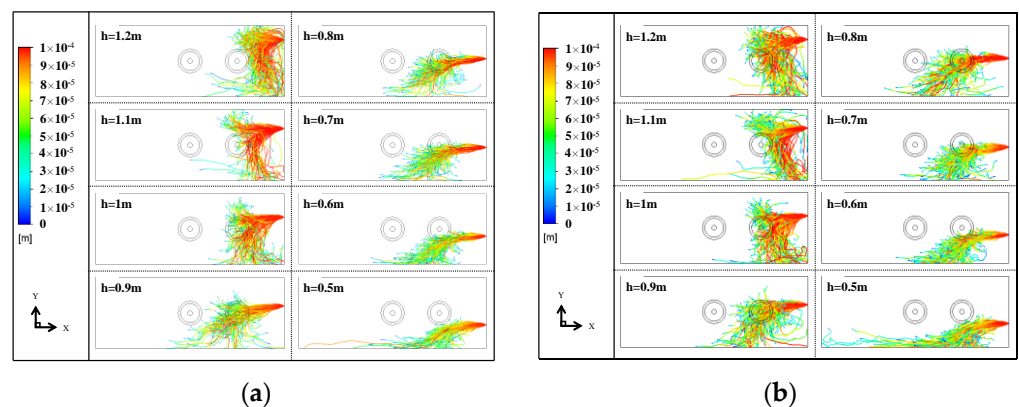


Figure 12. Change of droplet size with trajectory under different nozzle arrangement heights ($Z = 1.5$ m). (a) The burner is symmetrically arranged with reverse swirl. (b) Symmetrical arrangement of burners with same direction flow.

4. Conclusions

- (1) The symmetrical arrangement of burners is more conducive to the combustion of landfill leachate in the incinerator. For the three arrangements of burners (symmetrical arrangement of reverse swirl, symmetrical arrangement of same direction swirl, staggered arrangement of same direction flow), the outlet temperatures of flue gas are 1152.69 K, 1153.20 K, 1157.87 K, respectively, which are greater than 1123.15 K, meeting the temperature requirements in “3T+E” principle. However, only when the burners are symmetrically arranged, the residence time of the flue gas in the second combustion chamber can exceed 2 s, which meets the requirements of “3T+E” principle, so only the layout of burners should be symmetrical.
- (2) When the nozzle arrangement height is 0.9–0.8 m, it is more conducive to the combustion of landfill leachate. Only when the nozzle arrangement height is slightly higher than the center line of a combustion chamber (0.9–0.8 m) can the situation of concentrated liquid droplets rising with the flow field and concentrated liquid droplets being rolled to the bottom of a combustion chamber and hitting the wall with the reflux flue gas be avoided so as to reduce the wall-hitting ratio of the concentrated liquid and complete evaporative combustion.

Author Contributions: Conceptualization and writing—original draft preparation, W.W.; methodology and software, J.L.; mathematical model validation and data collation, S.G.; formal analysis, Z.Z.; investigation, G.C.; supervision and project administration, Z.Y. All authors have read and agreed to the published version of the manuscript.

Funding: This research was funded by [Chongqing Science and Technology Bureau] grant number [cstc2020jcyj-bshX0045].

Institutional Review Board Statement: Not applicable.

Informed Consent Statement: Not applicable.

Data Availability Statement: Not applicable.

Conflicts of Interest: The authors declare no conflict of interest.

References

1. Wang, C.; Sun, X.; Shan, H.; Naji, H.; Zhang, H.; Xi, B. Degradation of Landfill Leachate Using UV-TiO₂ Photocatalysis Combination with Aged Waste Reactors. *Processes* **2021**, *9*, 946. [[CrossRef](#)]
2. Jagaba, A.H.; Kutty, S.R.M.; Lawal, I.M.; Abubakar, S.; Hassan, I.; Zubairu, I.; Umaru, I.; Abdurrasheed, A.S.; Adam, A.A.; Ghaleb, A.A.S.; et al. Sequencing batch reactor technology for landfill leachate treatment: A state-of-the-art review. *J. Environ. Manag.* **2021**, *182*, 111946. [[CrossRef](#)] [[PubMed](#)]
3. Zhang, L.; Li, A.; Lu, Y.; Yan, L.; Zhong, S.; Deng, C. Characterization and removal of dissolved organic matter (DOM) from landfill leachate rejected by nanofiltration. *Waste Manag.* **2009**, *29*, 1035–1040. [[CrossRef](#)] [[PubMed](#)]
4. Keen, O.S. Characterisation of ultraviolet-absorbing recalcitrant organics in landfill leachate for treatment process optimisation. *Waste Manag. Res.* **2016**, *35*, 325–328. [[CrossRef](#)]
5. Wiszniowski, J.; Robert, J.; Surmacz-Gorska, J.; Miksch, K.; Weber, J.V. Landfill leachate treatment methods: A review. *Environ. Chem. Lett.* **2006**, *4*, 51–61. [[CrossRef](#)]
6. Akkaya, E.; Demir, A.; Karadag, D.; Varank, G.; Sinan Bilgili, M.; Ozkaya, B. Post-treatment of anaerobically treated medium-age landfill leachate. *Environ. Prog. Sustain. Energy* **2010**, *29*, 78–84. [[CrossRef](#)]
7. Renou, S.; Givaudan, J.G.; Poulain, S.; Dirassouyan, F.; Moulin, P. Landfill leachate treatment: Review and opportunity. *J. Hazard. Mater.* **2008**, *150*, 468–493. [[CrossRef](#)]
8. Šourková, M.; Adamcová, D.; Zloch, J.; Skutnik, Z.; Daria Vaverková, M. Thermal Stress and Deformation of Hollow Paddle-Shaft Components with Internal High Temperature Molten Salt Flow. *Environments* **2020**, *7*, 111. [[CrossRef](#)]
9. Seo, D.J.; Kim, Y.J.; Ham, S.Y.; Lee, D.H. Characterization of dissolved organic matter in leachate discharged from final disposal sites which contained municipal solid waste incineration residues. *J. Hazard. Mater.* **2007**, *148*, 679–692. [[CrossRef](#)]
10. Zhan, X.; Chen, Z.; Zhao, P. Rapid decomposition method of landfill leachate in recycling stations. *J. Environ. Biol.* **2019**, *40*, 448–459. [[CrossRef](#)]
11. Banch, T.J.; Hanafiah, M.M.; Alkarkhi, A.F.; Amr, S.S.; Nizam, N.U. Evaluation of Different Treatment Processes for Landfill Leachate Using Low-Cost Agro-Industrial Materials. *Processes* **2020**, *8*, 111. [[CrossRef](#)]

12. Chen, G.; Wu, G.; Li, N.; Lu, X.; Zhao, J.; He, M.; Yan, B.; Zhang, H.; Duan, X.; Wang, S. Landfill leachate treatment by persulphate related advanced oxidation technologies. *J. Hazard. Mater.* **2021**, *418*, 126355. [[CrossRef](#)] [[PubMed](#)]
13. Hong, S.K.; Dong, S.K.; Han, J.O.; Lee, J.S.; Lee, Y.C. Numerical study of effect of operating and design parameters for design of steam reforming reactor. *Energy* **2013**, *61*, 410–418. [[CrossRef](#)]
14. Rahimipetroudi, I.; Rashid, K.; Yang, J.B.; Dong, S.K. Comprehensive study of the effect of a developed co-firing burner and its front-wall, opposed-wall, and tangential firing arrangements on the performance improvement and emissions reduction of coal-natural gas combustion in a boiler. *Int. J. Therm. Sci.* **2022**, *173*, 10739. [[CrossRef](#)]
15. Mohammadpour, K.; Alkhalaf, A.M.R.; Chitsazan, A.; Specht, E. The CFD simulation of reactive flow in parallel flow regenerative shaft kilns using porous media model. *Therm. Sci.* **2021**, *26*, 281. [[CrossRef](#)]
16. Rohini, A.K.; Choi, S.H.; Lee, H.J. Numerical parametric study on the burner arrangement design for hydrogen production in a steam methane reformer. *Int. J. Energy Res.* **2021**, *45*, 16006–16026. [[CrossRef](#)]
17. Li, Z.; Qiao, X.; Miao, Z. A novel burner arrangement scheme with annularly combined multiple airflows for wall-tangentially fired pulverized coal boiler. *Energy* **2021**, *222*, 119912. [[CrossRef](#)]
18. Jing, L.; Zhao, J.; Wang, H.; Li, W.; Du, Y.; Zhu, Q.; Zayed, M.E. Numerical analysis of the effect of swirl angle and fuel equivalence ratio on the methanol combustion characteristics in a swirl burner. *Process Saf. Environ. Prot.* **2022**, *158*, 320–330. [[CrossRef](#)]
19. Ghasemi, H.M.; Gilani, N.; Daryan, J.T. Investigating the Effect of Fuel Rate Variation in an Industrial Thermal Cracking Furnace with Alternative Arrangement of Wall Burners Using Computational Fluid Dynamics Simulation. *J. Therm. Sci. Eng. Appl.* **2017**, *9*, 41012. [[CrossRef](#)]
20. Ehrhardt, K.; Ehret, A.; Leuckel, W. Experimental study on the dependence of burnout on the operation conditions and physical properties in wastewater incineration. *Symp. Int. Combust.* **1998**, *27*, 1293–1299. [[CrossRef](#)]
21. Bai, Y.; Bao, Y.B.; Cai, X.L.; Chen, C.H.; Ye, X.C. Feasibility of disposing waste glyphosate neutralization liquor with cement rotary kiln—ScienceDirect. *J. Hazard. Mater.* **2014**, *278*, 500–505. [[CrossRef](#)] [[PubMed](#)]
22. Liu, Y.; Mendoza-Perilla, P.; Clavier, K.A.; Tolaymat, T.M.; Bowden, J.A.; Solo-Gabriele, H.M.; Townsend, T.G. Municipal solid waste incineration (MSWI) ash co-disposal: Influence on per- and polyfluoroalkyl substances (PFAS) concentration in landfill leachate. *Waste Manag.* **2022**, *144*, 49–56. [[CrossRef](#)] [[PubMed](#)]
23. Zhang, W.; Wang, S. Thermal degradation and kinetic analysis of organic constituents in coal-gasification wastewater with a novel treatment. *Int. J. Low-Carbon Technol.* **2020**, *15*, 620–628. [[CrossRef](#)]